Chemical Engineering Journal 149 (2009) 435–446

Contents lists available at ScienceDirect

Chemical Engineering Journal

journal homepage: www.elsevier.com/locate/cej

Proactive product quality control: An integrated product and process control approach to MIMO systems

Zheng Liu, Jie Xiao, Yinlun Huang*

Department of Chemical Engineering and Materials Science, Wayne State University, 5050 Anthony Wayne Drive, Detroit, MI 48202, USA

ARTICLE INFO

Article history:
Received 6 October 2008
Received in revised form 6 February 2009
Accepted 10 February 2009

Keywords:
Product quality control
Process control
Integrated product and process engineering
Multi-input–multi-output system

ABSTRACT

Real-time control of product performance parameters is a key for proactive quality control (QC), as it can prevent the occurrence of potential quality problems in the earliest stage of manufacturing. It is recognized that dynamic product QC must be coordinated with the control of the process through which the product is manufactured. The integrated product and process control (IPPC) design methodology introduced recently is a proven approach to the simultaneous control of both the product quality and the process performance. In this paper, a general IPPC design methodology for multi-input–multi-output (MIMO) systems is introduced. A case study on polymeric coating curing shows that the resulting control system is capable of effectively tracking the set-points of both the product and the process, and demonstrating a satisfactory performance in rejecting disturbances, thereby ensuring achievement of desirable product quality and process performance.

1. Introduction

Product quality control (QC) is traditionally realized through post-process quality inspection in most manufacturing systems. In practice, after a quality problem is identified in the products, a statistical analysis is usually conducted and the relevant process operational settings are then adjusted to prevent the same type of problems from reoccurrence. This type of QC, although necessary in manufacturing, is reactive in nature as it "waits for" the appearance of quality problems first. It is also ineffective since a significant time lag may exist from problem identification, through solution derivation, to action taking. Note that during this time period, the same type of quality problems can continuously appear in many products being manufactured. Furthermore, the derived solutions are frequently heuristic in nature, which may lead to problem solving not always effective.

In modern manufacturing, product quality standard becomes increasingly high, which makes process operation more challenging. Thus, traditional inspection-based QC alone is no longer sufficient in quality assurance. QC must be fundamentally proactive, aiming at quality assurance starting from the earliest stage of product manufacturing. In 1989, Wu et al. introduced a QC concept called the New Generation Quality Control [1]. Its essential element is an implementation of reliable real-time process control. Yabuki and MacGregor suggested a practical approach, called midcourse correction, to control the final product quality for a semi-batch reactor [2]. Lou and Huang extended the idea and introduced an integrated process and product dynamic modeling approach, which facilitates simultaneous control of both process and product [3]. Recently, Xiao et al. introduced a concept of integrated product and process control (IPPC) and a target-oriented control system design methodology [4]. It is shown that IPPC is an effective approach to realizing all-time on-aim proactive product QC. However, the method is limited to single-input–single-output (SISO) linear systems, while most manufacturing systems are nonlinear and have multiple product quality and process performance parameters.

In this paper, the IPPC concept by Xiao et al. is adopted, but the IPPC system design methodology is extended for controlling multi-input–multi-output (MIMO) product–process systems. A case study will show that the resulting control system is capable of effectively tracking the set-points of both the product and the process, and demonstrating a satisfactory performance in rejecting disturbances exerted on them, thereby ensuring both desirable product quality and superior process performance.

2. Proactive quality control essential

The effectiveness of product QC, regardless of the approaches and strategies used, is reflected by the satisfaction of the defined quality criteria. If $\boldsymbol{Q}$ is the vector of quality indicators for product P, then $\boldsymbol{Q}(P)$ is the vector of the assessed quality indicator values. Let $\boldsymbol{Q}_L(P)$ and $\boldsymbol{Q}_H(P)$ be, respectively, the lowest and the highest

* Corresponding author. Tel.: +1 313 577 3771; fax: +1 313 577 3810.
E-mail address: yhuang@wayne.edu (Y. Huang).

1385-8947/$ – see front matter © 2009 Elsevier B.V. All rights reserved.
doi:10.1016/j.cej.2009.02.007

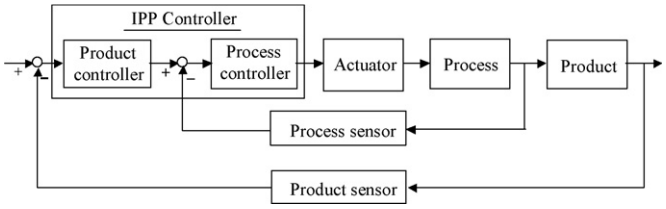

Fig. 1. General scheme for IPP control [4].

acceptable values of the quality indicators. The product has a satisfactory quality, if the following condition is satisfied:

$$\boldsymbol{Q}_L(P) \le \boldsymbol{Q}(P) \le \boldsymbol{Q}_H(P) \tag{1}$$

The above approach has been commonly used in post-process quality inspection activities.

2.1. Dynamic QC

In IPPC control design, a key component is the dynamic characterization of a product that is being manufactured. This requires product dynamic modeling, in addition to usual process dynamic modeling. The resulting models should generate the dynamic information of the process outputs, $\boldsymbol{Y}_c(t)$, and the product outputs, $\boldsymbol{Y}_d(t)$, which can be described as

$$\boldsymbol{Y}_c(t) = g(\boldsymbol{X}_c(t), \boldsymbol{U}_c(t), \boldsymbol{Z}_c(t), t) \tag{2}$$

$$\boldsymbol{Y}_d(t) = f(\boldsymbol{X}_d(t), \boldsymbol{U}_d(t), \boldsymbol{Z}_d(t), t) \tag{3}$$

where $\boldsymbol{X}_c(t)$ is the process state vector; $\boldsymbol{U}_c(t)$ is the process control vector; $\boldsymbol{Z}_c(t)$ is the process disturbance vector; $\boldsymbol{X}_d(t)$ is the product state vector; $\boldsymbol{Z}_d(t)$ is the product disturbance vector; $\boldsymbol{U}_d(t)$ is the product control vector and, in reality, is the process output vector, $\boldsymbol{Y}_c(t)$. Eq. (3) can be rewritten as,

$$\boldsymbol{Y}_d(t) = f(\boldsymbol{X}_d(t), \boldsymbol{Y}_c(t), \boldsymbol{Z}_d(t), t) \tag{4}$$

Extended from the static to the dynamic domain, the product quality vector can be written as

$$\boldsymbol{Q}(P, t) = h(\boldsymbol{Y}_d(t), t) \tag{5}$$

According to Eqs. (2) and (3), the above equation can be further written as,

$$\boldsymbol{Q}(P, t) = h(\boldsymbol{X}_d(t), \boldsymbol{X}_c(t), \boldsymbol{U}_c(t), \boldsymbol{Z}_d(t), \boldsymbol{Z}_c(t), t) \tag{6}$$

Note that $\boldsymbol{Q}(P)$ in Eq. (1) quantifies the product quality at the ending time (t_e) of a product manufacturing process, i.e., $\boldsymbol{Q}(P, t_e)$. Clearly, to realize proactive QC, dynamic cause-effect relationships for the process and the product should be established, and control strategies should be developed.

2.2. IPPC scheme

The IPPC–SISO design by Xiao et al. [4] employs a cascade control scheme. As shown in Fig. 1, the inner loop of the system is for process control, while the outer loop is for product control. The integrated process and product (IPP) controller of the system is an integration of a product controller and a process controller. The product controller functions based on the error between its set-point and the measured product controlled variable; it dynamically adjusts the set-point to the process controller. The output of the IPP controller is used to control the process through the process actuator, and in turn the product being manufactured. This scheme is general for a system with any number of inputs and outputs, and is extended for IPPC of MIMO systems in this work.

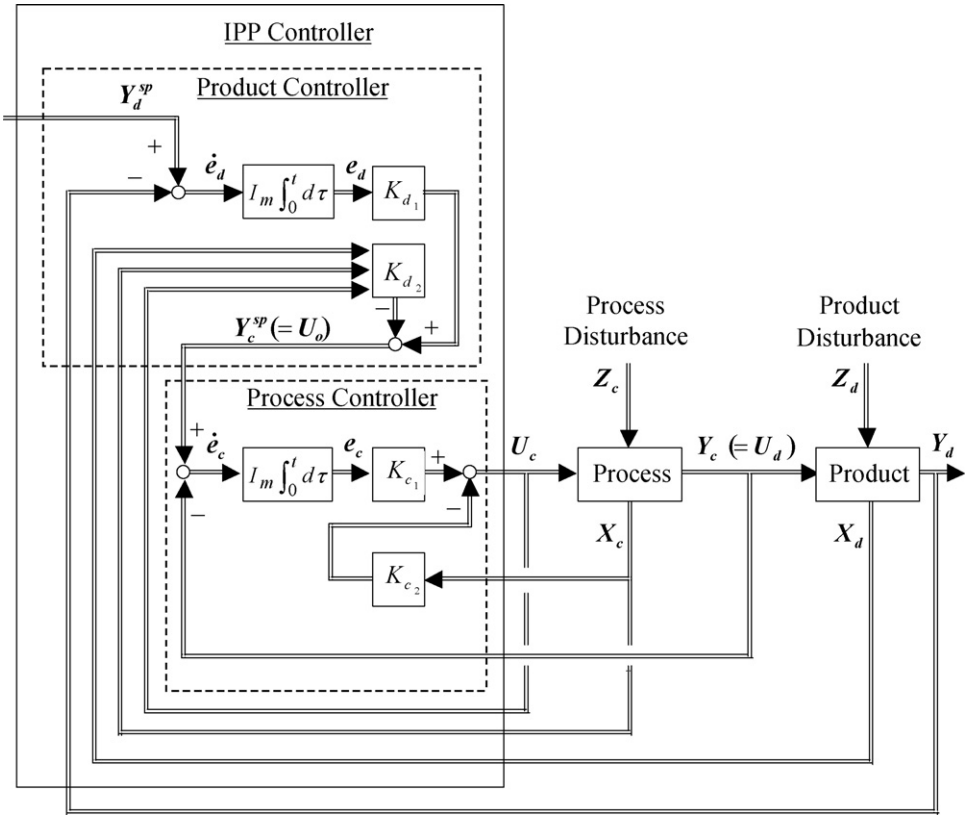

Fig. 2. IPP control system design for MIMO systems.

3. System design

Fig. 2 depicts a general IPPC–MIMO system structure, which adopts the cascade control scheme. In this system, the process system and the product system each are assumed to be satisfactorily described by linear state-space models, and, further, full state/output feedback control is assumed to be realizable [5,6]. In the control system, each controller is composed of an integrator and two gain matrices. Thus, the IPP control design is mainly the design of all four gain matrices ($\boldsymbol{K}_{c_1}$, $\boldsymbol{K}_{c_2}$, $\boldsymbol{K}_{d_1}$, and $\boldsymbol{K}_{d_2}$) based on the characteristics of the process and the product, the control objective(s), etc. A logic design of the system is to determine the gain matrices for the inner loop first, and those for the outer loop later.

3.1. System modeling

The process and the product are described by the following linear models.

3.1.1. Process model

A linear process model is

$$\dot{\boldsymbol{X}}_c = \boldsymbol{A}_c\boldsymbol{X}_c + \boldsymbol{B}_c\boldsymbol{U}_c \tag{7}$$

$$\boldsymbol{Y}_c = \boldsymbol{C}_c\boldsymbol{X}_c + \boldsymbol{D}_c\boldsymbol{Z}_c \tag{8}$$

where $\boldsymbol{X}_c$ is the process state vector ($n \times 1$); $\boldsymbol{U}_c$ the process control vector ($m \times 1$); $\boldsymbol{Y}_c$ the process controlled (or output) vector ($m \times 1$); $\boldsymbol{A}_c$ the process system matrix ($n \times n$); $\boldsymbol{B}_c$ the process control matrix ($n \times m$); $\boldsymbol{C}_c$ the process output coefficient matrix ($m \times n$); $\boldsymbol{D}_c$ the process disturbance coefficient matrix ($m \times k$); $\boldsymbol{Z}_c$ the process disturbance vector ($k \times 1$).

3.1.2. Product model

Similarly, a linear product system can be written as

$$\dot{\boldsymbol{X}}_d = \boldsymbol{A}_d\boldsymbol{X}_d + \boldsymbol{B}_d\boldsymbol{U}_d \tag{9}$$

$$\boldsymbol{Y}_d = \boldsymbol{C}_d\boldsymbol{X}_d + \boldsymbol{D}_d\boldsymbol{Z}_d \tag{10}$$

where $\boldsymbol{X}_d$ is the product state vector ($l \times 1$); $\boldsymbol{U}_d$ the product control vector ($m \times 1$), which is essentially the process output vector $\boldsymbol{Y}_c$; $\boldsymbol{Y}_d$ the product controlled (or output) vector ($m \times 1$); $\boldsymbol{A}_d$ the product system matrix ($l \times l$); $\boldsymbol{B}_d$ the product control matrix ($l \times m$); $\boldsymbol{C}_d$ the product output coefficient vector ($m \times l$); $\boldsymbol{D}_d$ the product disturbance coefficient matrix ($m \times j$); $\boldsymbol{Z}_d$ the product disturbance vector ($j \times 1$).

3.2. Process control loop design

As shown in Fig. 2, the inner loop is a standard state-output feedback control system using a PI controller. With a standard integral module, the design of this controller is essentially the determination of the two gain matrices, $\boldsymbol{K}_{c_1}$ and $\boldsymbol{K}_{c_2}$.

Miron introduced a design method for parameter determination for a state-output feedback control system [7], which is to transform such a system to the one with state feedback. This approach is adopted in this work; the detailed derivation of gain matrices for the process controller is given in Appendix A. The final controller gain matrices can be evaluated by the following equation.

$$\begin{pmatrix} \boldsymbol{K}_{c_1} & \boldsymbol{K}_{c_2} \end{pmatrix} = \boldsymbol{K}_c^p \begin{pmatrix} \boldsymbol{C}_c & \boldsymbol{0} \\ \boldsymbol{A}_c & \boldsymbol{B}_c \end{pmatrix}^{-1} \tag{11}$$

Note that matrices $\boldsymbol{A}_c$, $\boldsymbol{B}_c$, and $\boldsymbol{C}_c$ are given in the process system model in Eqs. (7) and (8). Matrix $\boldsymbol{K}_c^p$ is a preferred system behavior matrix. A method for determining $\boldsymbol{K}_c^p$ is introduced later.

3.3. Process-embedded product control loop design

The design approach for the inner loop of the IPPC system is applicable to the design of the outer loop, except that the designed inner loop will be treated as a functional block that is placed in series with the open product block. The product model can be derived as

$$\begin{pmatrix} \dot{\boldsymbol{\Psi}}_c \\ \dot{\boldsymbol{X}}_d \end{pmatrix} = \begin{pmatrix} \boldsymbol{\Lambda}_c - \boldsymbol{\Gamma}_c\boldsymbol{K}_c^p & \boldsymbol{0} \\ \boldsymbol{B}_d\boldsymbol{\Omega}_c & \boldsymbol{A}_d \end{pmatrix} \begin{pmatrix} \boldsymbol{\Psi}_c \\ \boldsymbol{X}_d \end{pmatrix} + \begin{pmatrix} \boldsymbol{\Gamma}_c \\ \boldsymbol{0} \end{pmatrix} \boldsymbol{\Phi}_c^{sp} + \begin{pmatrix} \boldsymbol{0} \\ \boldsymbol{B}_d\boldsymbol{D}_c \end{pmatrix} \boldsymbol{Z}_c \tag{12}$$

where

$$\boldsymbol{\Psi}_c = \begin{pmatrix} \boldsymbol{X}_c \\ \boldsymbol{U}_c \end{pmatrix} \tag{13}$$

$$\boldsymbol{\Phi}_c^{sp} = \boldsymbol{K}_{c_1} \begin{pmatrix} \boldsymbol{I}_m & -\boldsymbol{D}_c \end{pmatrix} \begin{pmatrix} \boldsymbol{Y}_c^{sp} \\ \boldsymbol{Z}_c \end{pmatrix} \tag{14}$$

$$\boldsymbol{\Lambda}_c = \begin{pmatrix} \boldsymbol{A}_c & \boldsymbol{B}_c \\ 0 & 0 \end{pmatrix} \tag{15}$$

$$\boldsymbol{\Gamma}_c = \begin{pmatrix} 0 \\ \boldsymbol{I}_m \end{pmatrix} \tag{16}$$

$$\boldsymbol{K}_c^p = \begin{pmatrix} \boldsymbol{K}_{c_1}\boldsymbol{C}_c + \boldsymbol{K}_{c_2}\boldsymbol{A}_c & \boldsymbol{K}_{c_2}\boldsymbol{B}_c \end{pmatrix} \tag{17}$$

Correspondingly, the system output model in Eq. (8) can be rewritten as

$$\boldsymbol{Y}_c = \boldsymbol{\Omega}_c\boldsymbol{\Psi}_c + \boldsymbol{D}_c\boldsymbol{Z}_c \tag{18}$$

where

$$\boldsymbol{\Omega}_c = \begin{pmatrix} \boldsymbol{C}_c & 0 \end{pmatrix} \tag{19}$$

Note that vectors $\boldsymbol{Y}_c$ and $\boldsymbol{U}_d$ are equivalent (see, Fig. 2). Thus, the product output model in Eq. (10) becomes:

$$\boldsymbol{Y}_d = \begin{pmatrix} 0 & \boldsymbol{C}_d \end{pmatrix} \begin{pmatrix} \boldsymbol{\Psi}_c \\ \boldsymbol{X}_d \end{pmatrix} + \boldsymbol{D}_d\boldsymbol{Z}_d \tag{20}$$

The models in Eqs. (12) and (20) can be rewritten more concisely as follows, which is essentially a closed-loop-process-open-loop-product model:

$$\dot{\boldsymbol{X}}_o = \boldsymbol{A}_o\boldsymbol{X}_o + \boldsymbol{B}_o\boldsymbol{U}_o + \boldsymbol{E}_o\boldsymbol{Z}_c \tag{21}$$

$$\boldsymbol{Y}_o = \boldsymbol{C}_o\boldsymbol{X}_o + \boldsymbol{D}_o\boldsymbol{Z}_o \tag{22}$$

where

$$\boldsymbol{X}_o = \begin{pmatrix} \boldsymbol{\Psi}_c \\ \boldsymbol{X}_d \end{pmatrix} \tag{23}$$

$$\boldsymbol{Y}_o = \boldsymbol{Y}_d \tag{24}$$

$$\boldsymbol{Z}_o = \boldsymbol{Z}_d \tag{25}$$

$$\boldsymbol{U}_o = \boldsymbol{\Phi}_c^{sp} \tag{26}$$

$$\boldsymbol{A}_o = \begin{pmatrix} \boldsymbol{\Lambda}_c - \boldsymbol{\Gamma}_c\boldsymbol{K}_c^p & 0 \\ \boldsymbol{B}_d\boldsymbol{\Omega}_c & \boldsymbol{A}_d \end{pmatrix} \tag{27}$$

$$\boldsymbol{B}_o = \begin{pmatrix} \boldsymbol{\Gamma}_c \\ 0 \end{pmatrix} \tag{28}$$

$$\boldsymbol{C}_o = \begin{pmatrix} 0 & \boldsymbol{C}_d \end{pmatrix} \tag{29}$$

$$\boldsymbol{D}_o = \boldsymbol{D}_d \tag{30}$$

$$\boldsymbol{E}_o = \begin{pmatrix} 0 \\ \boldsymbol{B}_d \boldsymbol{D}_c \end{pmatrix} \tag{31}$$

Similar to the process controller design, the product controller can be designed for this process-integrated product system. The detailed derivation of the product controller gain matrices is given in Appendix B, with the final results as follows:

$$\begin{pmatrix} \boldsymbol{K}_{d_1} & \boldsymbol{K}_{d_2} \end{pmatrix} = \boldsymbol{K}_d^p \begin{pmatrix} \boldsymbol{C}_o & \boldsymbol{0} \\ \boldsymbol{A}_o & \boldsymbol{B}_o \end{pmatrix}^{-1} \tag{32}$$

Note that the controller gain matrices are determined by the preferred system behavior matrix $\boldsymbol{K}_d^p$; a method for determining this matrix is presented in the next section.

3.4. Preferred system behavior matrix determination

As shown in Appendix A, the closed-loop process system can be derived as,

$$\dot{\boldsymbol{\Psi}}_c = (\boldsymbol{\Lambda}_c - \boldsymbol{\Gamma}_c \boldsymbol{K}_c^p)\boldsymbol{\Psi}_c + \boldsymbol{\Gamma}_c \boldsymbol{\Phi}_c^{sp}$$

where the variables and parametric matrices are defined in Eqs. (13) through (17). The system's output model is given in Eq. (18). Also, according to Appendix B, the closed-loop product system is modeled as:

$$\dot{\boldsymbol{\Psi}}_d = (\boldsymbol{\Lambda}_d - \boldsymbol{\Gamma}_d \boldsymbol{K}_d^p)\boldsymbol{\Psi}_d + \boldsymbol{\Gamma}_d \boldsymbol{\Phi}_d^{sp} + \boldsymbol{E}_d \boldsymbol{Z}_c$$

$$\boldsymbol{Y}_d = \boldsymbol{\Omega}_d \boldsymbol{\Psi}_d + \boldsymbol{D}_d \boldsymbol{Z}_d$$

Note that the preferred system behavior matrices ($\boldsymbol{K}_c^p$ and $\boldsymbol{K}_d^p$) contained in Eqs. (A6) and (B5) are the state gain matrices which can be determined by a closed-loop pole placement method.

The pole placement for an MIMO system is considerably more complicated than that for an SISO system. Miron [7] introduced a general mathematical framework for determining a preferred gain matrix for a state feedback MIMO control system (see Fig. 3); the method is adopted in this work for selecting $\boldsymbol{K}_c^p$ and $\boldsymbol{K}_d^p$. To facilitate reader's understanding, a 2×2 system is used to illustrate the method below. A more general method should be referred to Miron [7].

3.4.1. Control system state-space model

For a 2×2 process or product system stated in Eq. (7) or (9), respectively, a general controllable pair $(\boldsymbol{A}, \boldsymbol{B})$ is

$$\boldsymbol{A} = \begin{pmatrix} a_{11} & a_{12} \\ a_{21} & a_{22} \end{pmatrix} \tag{33}$$

$$\boldsymbol{B} = \begin{pmatrix} b_{11} & b_{12} \\ b_{21} & b_{22} \end{pmatrix} \tag{34}$$

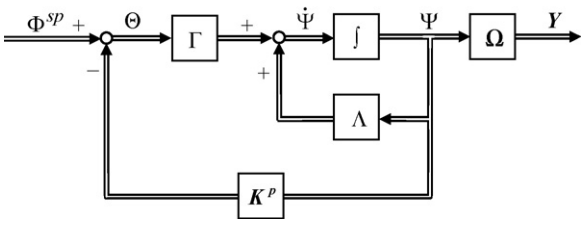

Fig. 3. A standard state feedback control system.

According to Eqs. (15) and (16), the controllable pair in an equivalent state-feedback-only system is $(\boldsymbol{\Lambda}, \boldsymbol{\Gamma})$, which is defined as

$$\boldsymbol{\Lambda} = \begin{pmatrix} a_{11} & a_{12} & b_{11} & b_{12} \\ a_{21} & a_{22} & b_{21} & b_{22} \\ 0 & 0 & 0 & 0 \\ 0 & 0 & 0 & 0 \end{pmatrix} \tag{35}$$

$$\boldsymbol{\Gamma} = \begin{pmatrix} 0 & 0 \\ 0 & 0 \\ 1 & 0 \\ 0 & 1 \end{pmatrix} \tag{36}$$

It is shown that this system has four state variables ($n = 4$) and two input variables ($m = 2$).

3.4.2. Transformation matrix construction

To facilitate a pole placement, system matrices Λ and Γ need to be transformed into a block-controllable form, which are denoted as $\boldsymbol{\Lambda}^B$ and $\boldsymbol{\Gamma}^B$, respectively. This requires the development of a transformation matrix denoted as $\boldsymbol{T}$. In this regard, a controllability test matrix denoted as $\boldsymbol{C}_t$ must be constructed for the pair $(\boldsymbol{\Lambda}, \boldsymbol{\Gamma})$, i.e.,

$$\boldsymbol{C}_t = \begin{pmatrix} 0 & 0 & b_{11} & b_{12} & \cdots \\ 0 & 0 & b_{21} & b_{22} & \cdots \\ 1 & 0 & 0 & 0 & \cdots \\ 0 & 1 & 0 & 0 & \cdots \end{pmatrix} \tag{37}$$

Note that since the system has four state variables ($n = 4$), only the first four columns in Eq. (37) are listed for use. Then, a selection matrix, namely $\boldsymbol{S}$, should be generated by constructing a 2×2 identity matrix (since $m = 2$) repeatedly until the column count reaches 4 (since $n = 4$); this yields,

$$\boldsymbol{S} = \begin{pmatrix} 1 & 0 & 1 & 0 \\ 0 & 1 & 0 & 1 \end{pmatrix} \tag{38}$$

According to Miron [7], another matrix, denoted as $\boldsymbol{F}$, should be then constructed by rearranging the sequence of the first four columns of $\boldsymbol{C}_t$ so that all columns belonging to a particular input are made together in a group (i.e., sub-matrix). The following two-step procedure is described for constructing matrix $\boldsymbol{F}$.

Step 1. Start from the first row of matrix $\boldsymbol{S}$ to identify the column numbers of the elements with the value of 1 in that row.
Step 2. Use the column numbers obtained in Step 1 to collect the columns in $\boldsymbol{C}_t$ and then add these column elements as a sub-matrix into the left most unfilled columns in matrix $\boldsymbol{F}$.

The two-step procedure should be ended when all the rows of matrix $\boldsymbol{S}$ are checked. The resulting matrix $\boldsymbol{F}$ should have the following structure:

$$\boldsymbol{F} = \begin{pmatrix} 0 & b_{11} & 0 & b_{12} \\ 0 & b_{21} & 0 & b_{22} \\ 1 & 0 & 0 & 0 \\ 0 & 0 & 1 & 0 \end{pmatrix} \tag{39}$$

The above matrix consists of two sub-matrices; the first two columns ($n_1 = 2$) form the first sub-matrix, which belongs to the first system input, and the next two columns ($n_2 = 2$) form the second sub-matrix, which belongs to the second system input. Taking an

inverse of matrix $\boldsymbol{F}$ yields:

$$\boldsymbol{F}^{-1} = \begin{pmatrix} \boldsymbol{f}_1 \\ \boldsymbol{f}_2 \\ \boldsymbol{f}_3 \\ \boldsymbol{f}_4 \end{pmatrix} = \begin{pmatrix} 0 & 0 & 1 & 0 \\ \dfrac{b_{22}}{|\boldsymbol{B}|} & -\dfrac{b_{12}}{|\boldsymbol{B}|} & 0 & 0 \\ 0 & 0 & 0 & 1 \\ -\dfrac{b_{21}}{|\boldsymbol{B}|} & \dfrac{b_{11}}{|\boldsymbol{B}|} & 0 & 0 \end{pmatrix} \begin{matrix} \\ \} n_1 \text{ rows} \\ \\ \} n_2 \text{ rows} \end{matrix} \tag{40}$$

where

$$|\boldsymbol{B}| = b_{11}b_{22} - b_{12}b_{21} \tag{41}$$

Matrices $\boldsymbol{\Lambda}$ in Eq. (35) and $\boldsymbol{F}^{-1}$ in Eq. (40) are used to construct transformation matrix $\boldsymbol{T}$ in the following way. The n_1-th row in $\boldsymbol{F}^{-1}$ (i.e., $\boldsymbol{f}_2$) is used to generate the first n_1 rows in $\boldsymbol{T}$ and the $(n_1 + n_2)$-th row in $\boldsymbol{F}^{-1}$ (i.e., $\boldsymbol{f}_4$) is used to generate the next n_2 rows in $\boldsymbol{T}$. This gives rise to the matrix in the following structure:

$$\boldsymbol{T} = \begin{pmatrix} \boldsymbol{f}_2 \\ \boldsymbol{f}_2\boldsymbol{\Lambda} \\ \boldsymbol{f}_4 \\ \boldsymbol{f}_4\boldsymbol{\Lambda} \end{pmatrix} = \begin{pmatrix} \dfrac{b_{22}}{|\boldsymbol{B}|} & -\dfrac{b_{12}}{|\boldsymbol{B}|} & 0 & 0 \\ \dfrac{a_{11}b_{22} - a_{21}b_{12}}{|\boldsymbol{B}|} & \dfrac{a_{12}b_{22} - a_{22}b_{12}}{|\boldsymbol{B}|} & 1 & 0 \\ -\dfrac{b_{21}}{|\boldsymbol{B}|} & \dfrac{b_{11}}{|\boldsymbol{B}|} & 0 & 0 \\ \dfrac{a_{21}b_{11} - a_{11}b_{21}}{|\boldsymbol{B}|} & \dfrac{a_{22}b_{11} - a_{12}b_{21}}{|\boldsymbol{B}|} & 0 & 1 \end{pmatrix} \begin{matrix} \\ \} n_1 \text{ rows} \\ \\ \} n_2 \text{ rows} \end{matrix} \tag{42}$$

3.4.3. Block-controllable state matrix

Matrix $\boldsymbol{T}$ is used to transform the system matrices $\boldsymbol{\Lambda}$ in Eq. (35) and $\boldsymbol{\Gamma}$ in Eq. (36) into the block-controllable form $\boldsymbol{\Lambda}^B$ and $\boldsymbol{\Gamma}^B$ below:

$$\boldsymbol{\Lambda}^B = \boldsymbol{T}\boldsymbol{\Lambda}\boldsymbol{T}^{-1} = \left(\begin{array}{cc:cc} 0 & 1 & 0 & 0 \\ \Lambda^B_{21} & \Lambda^B_{22} & \Lambda^B_{23} & \Lambda^B_{24} \\ \hdashline 0 & 0 & 0 & 1 \\ \Lambda^B_{41} & \Lambda^B_{42} & \Lambda^B_{43} & \Lambda^B_{44} \end{array}\right) = \begin{pmatrix} \boldsymbol{\Lambda}^{B,I} & \boldsymbol{\Lambda}^{B,II} \\ \boldsymbol{\Lambda}^{B,III} & \boldsymbol{\Lambda}^{B,IV} \end{pmatrix} \tag{43}$$

where the elements in the second and fourth rows can be readily calculated, whose explicit form are omitted here.

$$\boldsymbol{\Gamma}^B = \boldsymbol{T}\boldsymbol{\Gamma} = \left(\begin{array}{cc} 0 & 0 \\ 1 & 0 \\ \hdashline 0 & 0 \\ 0 & 1 \end{array}\right) \tag{44}$$

3.4.4. Preferred state gain matrix calculation

The feedback matrix ($\boldsymbol{K}^B$) for the system in a block-controllable form can be determined by assigning poles to each sub-system. As shown in Eq. (43), there are two second-order sub-systems (see $\boldsymbol{\Lambda}^{B,I}$ and $\boldsymbol{\Lambda}^{B,IV}$). Assuming the expected characteristic polynomial for each second-order system is $s^2 + \xi_1 s + \xi_2$, the preferred system matrix should be:

$$\boldsymbol{\Lambda}^B - \boldsymbol{\Gamma}^B\boldsymbol{K}^B = \left(\begin{array}{cc:cc} 0 & 1 & 0 & 0 \\ -\xi_2 & -\xi_1 & 0 & 0 \\ \hdashline 0 & 0 & 0 & 1 \\ 0 & 0 & -\xi_2 & -\xi_1 \end{array}\right) \tag{45}$$

Substituting Eqs. (43) and (44) into Eq. (45) and rearranging it yield:

$$\begin{pmatrix} 0 & 0 \\ 1 & 0 \\ 0 & 0 \\ 0 & 1 \end{pmatrix} \boldsymbol{K}^B = \begin{pmatrix} 0 & 0 & 0 & 0 \\ \Lambda^B_{21} + \xi_2 & \Lambda^B_{22} + \xi_1 & \Lambda^B_{23} & \Lambda^B_{24} \\ 0 & 0 & 0 & 0 \\ \Lambda^B_{41} & \Lambda^B_{42} & \Lambda^B_{43} + \xi_2 & \Lambda^B_{44} + \xi_1 \end{pmatrix} \tag{46}$$

According to Eq. (46), matrix $\boldsymbol{K}^B$ can be derived as follows:

$$\boldsymbol{K}^B = \begin{pmatrix} \Lambda^B_{21} + \xi_2 & \Lambda^B_{22} + \xi_1 & \Lambda^B_{23} & \Lambda^B_{24} \\ \Lambda^B_{41} & \Lambda^B_{42} & \Lambda^B_{43} + \xi_2 & \Lambda^B_{44} + \xi_1 \end{pmatrix} \tag{47}$$

The coefficients in the characteristic polynomial can be specified according to a preferred closed-loop dynamic response. In this work, the ITAE (Integral of Time-weighted Absolute Error) criterion is adopted. The objective function for choosing optimal controller parameter setting is to minimize the ITAE, which is expressed as [8]:

$$\text{ITAE} = \int_0^\infty t|e(t)|dt \tag{48}$$

Note that the controller parameters set in this way will give rise to a control system showing a relatively small overshoot with little oscillation as a response to step changes. According to Miron [7], the characteristic polynomial corresponds to a second-order system that minimizes the ITAE criterion is $s^2 + 1.4s + 1$ (see Table 1, where the parameters of the polynomials for a system with different orders are given as well). Thus, two variables ξ_1 and ξ_2 in matrix $\boldsymbol{K}^B$ should be 1.4 and 1, respectively.

Table 1
Transfer functions for minimum ITAE systems [7].

System with step input: $T(s) = 1/D(s) = 1/(s^n + a_{n-1}s^{n-1} + \cdots + a_1 s + 1)$		
n	a_i	Poles of $T(s)$
1	1, 1	1
2	1, 1.4, 1	$-0.7 \pm j0.7141$
3	1, 1.75, 2.15, 1	$-0.7081, -0.521 \pm j1.068$
4	1, 2.1, 3.4, 2.7, 1	$-0.626 \pm j0.414, -0.424 \pm j1.263$
5	1, 2.8, 5, 5.5, 3.4, 1	$-0.8955, -0.5758 \pm j0.5.339, -0.3764 \pm j1.292$

3.4.5. Reverse transformation

Since $\boldsymbol{K}^B$ is designed for a system in a block-controllable form, it should be transformed back to obtain the preferred state gain matrix $\boldsymbol{K}^p$ for the original system. According to Eqs. (43) and (44), the following relationship is evident:

$$\boldsymbol{\Lambda}^B - \boldsymbol{\Gamma}^B\boldsymbol{K}^B = \boldsymbol{T}\boldsymbol{\Lambda}\boldsymbol{T}^{-1} - \boldsymbol{T}\boldsymbol{\Gamma}\boldsymbol{K}^B = \boldsymbol{T}(\boldsymbol{\Lambda} - \boldsymbol{\Gamma}\boldsymbol{K}^B\boldsymbol{T})\boldsymbol{T}^{-1} \tag{49}$$

If the following relationship is chosen,

$$\boldsymbol{K}^p = \boldsymbol{K}^B\boldsymbol{T}, \tag{50}$$

then the system in a block-controllable form becomes a coordinate transformation of the original system, and the two systems have the same poles.

3.4.6. Procedure for determining the preferred state gain matrix

For the given controllable pair ($\boldsymbol{A}$, $\boldsymbol{B}$) of the state-output-feedback system shown in Eqs. (33) and (34), the preferred state gain matrix, $\boldsymbol{K}^p$, can be determined by following the procedure that is given in Fig. 4.

3.5. IPP controller gain matrix determination procedure

With the derivation above, a simple procedure for identifying the controller gain matrices is introduced below:

Step 1. Construct the process model in Eqs. (7) and (8) and the product model in Eqs. (9) and (10).

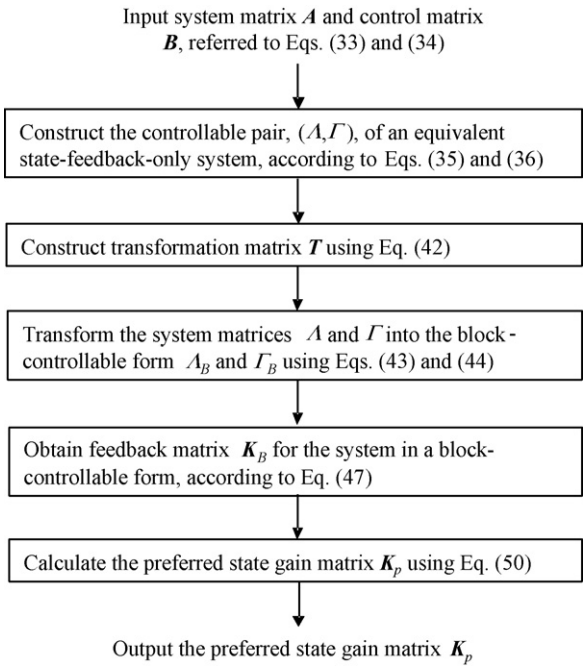

Fig. 4. Procedure for determining the preferred state gain matrix.

Step 2. Use the obtained process and product model to calculate the preferred state gain matrices $\boldsymbol{K}_c^p$ and $\boldsymbol{K}_d^p$ by following the five-step procedure given in Fig. 4.
Step 3. Calculate matrices $\boldsymbol{K}_{c_1}$ and $\boldsymbol{K}_{c_2}$ for the process controller in Eq. (11) and matrices $\boldsymbol{K}_{d_1}$ and $\boldsymbol{K}_{d_2}$ for the product controller in Eq. (32).

4. Case study on polymeric coating curing

The introduced IPPC design methodology is used to study an automotive coating curing problem. The objective of the study is to design an IPP control system so that the coating quality can be dynamically controlled under various types of disturbances exerted on the process-product system.

4.1. Process specification and system modeling

In automotive manufacturing, vehicle surface coating development is one of the most sophisticated operations in terms of its technical difficulty, energy and paint use efficiency, VOC emission and waste reduction. Among these, the most challenging problem is how to ensure coating quality. In production, vehicle bodies, when entering each baking oven, are covered by a thin layer of wet polymeric film. These vehicles loaded on a conveyor need to travel through the baking oven one by one at a constant speed for coating curing.

Fig. 5 shows a sketch of a usual baking oven. The oven, usually 120–250 m long, is divided into a number of operational zones, where the first one or two are designed as the radiation/convection zones and the rest are the convection-only zones. Each zone has different operational settings on wall temperature, convection air temperature and air volumetric flow rates. When a vehicle body travels through the oven, its panels are heated, which gives rise to the removal of the solvent contained in the wet film through evaporation, the change of the film thickness and topology, and the curing of the film through crosslinking reactions. Within a pre-set curing time, the curing process will be ended and the surface coating is

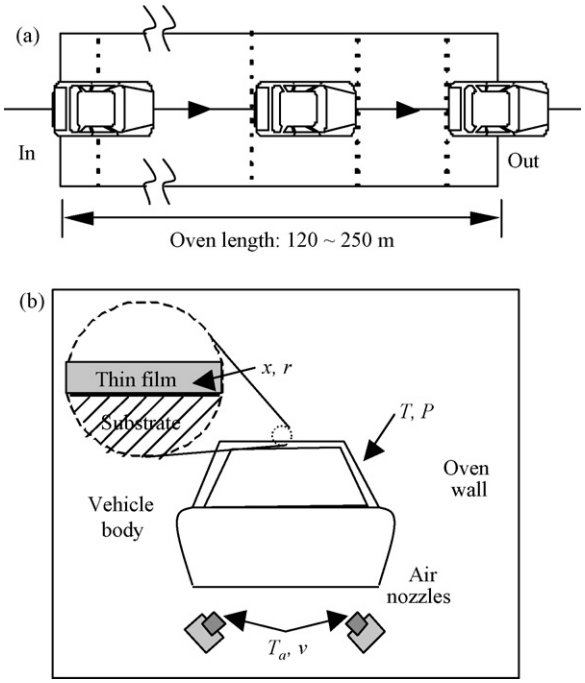

Fig. 5. Automotive coating curing system: (a) sketch of the coating curing process, and (b) illustration of the system parameters.

expected to achieve its desired quality. A detailed curing process description can be found in Lou and Huang [3].

According to Lou and Huang [3], Dickie et al. [9], and Peng [10], the curing process and the coating quality development are governed by the following nonlinear models:

$$\frac{dT}{dt} = \frac{a}{\rho_m C_{p_m} Z_m} v_{in}^{0.7}(T_a - T) \tag{51}$$

where T_a (K) is the convection air temperature, v_{in} (m/s) is the inlet convection air velocity, T (K) is the panel temperature, a is the heat transfer coefficient, and ρ_m (kg/m^3), C_{p_m} (J/kg K) and Z_m (m) are the density, the heat capacity, and the thickness of the metal substrate, respectively.

$$\frac{dP}{dt} = \frac{PA}{V}(v_{in} - v_{out}) \tag{52}$$

where P (Pa) is the air pressure within the oven, A (m^2) is the area of the ventilation openings at the inlet and outlet of the oven, and v_{out} (m/s) is the outlet convection air velocity.

$$\frac{dx}{dt} = \varsigma \exp\left(-\frac{E_r}{RT}\right)(1 - x) \tag{53}$$

where x (%) is the crosslinking conversion, E_r (J/mol) is the reaction activation energy, ς (1 s^{-1}) is the reaction frequency factor, and R is the gas constant (8.314 Pa m^3/mol K).

$$\frac{dr}{dt} = \frac{\beta}{m_0}\left(\alpha P - \exp\left(17.22 - \frac{3137}{T - 94.43}\right)(0.2r)^7\right) \tag{54}$$

where r (%) is the percentage of the solvent residue in the coating film, α (%) is the weight percentage of vapor phase within the drying air, β (kg/Pa s) is the mass transfer coefficient, and m_0 (kg) is the initial amount of solvent within the coating film.

The above nonlinear equations can be satisfactorily linearized to a 2 × 2 state-space model shown below.

4.1.1. Curing process model

The process input variables are the convection air temperature (T_a) and the inlet convection air velocity (v_{in}), and the process output variables are the panel temperature (T), which is assumed to be the polymeric film temperature, and the zone air pressure (P). The process model becomes:

$$\dot{\boldsymbol{X}}_c = \boldsymbol{A}_c\boldsymbol{X}_c + \boldsymbol{B}_c\boldsymbol{U}_c$$

$$\boldsymbol{Y}_c = \boldsymbol{C}_c\boldsymbol{X}_c + \boldsymbol{D}_c\boldsymbol{Z}_c$$

where

$$\boldsymbol{X}_c = \begin{pmatrix} T \\ P \end{pmatrix} \tag{55}$$

$$\boldsymbol{U}_c = \begin{pmatrix} T_a \\ v_{in} \end{pmatrix} \tag{56}$$

$$\boldsymbol{Y}_c = \begin{pmatrix} T \\ P \end{pmatrix} \tag{57}$$

$$\boldsymbol{Z_c} = \begin{pmatrix} z_c^T \\ z_c^P \end{pmatrix} \tag{58}$$

By using the parameter values given by Lou and Huang [3], the matrices have the following values:

$$\boldsymbol{A}_c = \begin{pmatrix} -0.0023 & 0 \\ 0 & -0.0025 \end{pmatrix} \tag{59}$$

$$\boldsymbol{B}_c = \begin{pmatrix} 0.023 & 0.04 \\ 0 & 1.667 \end{pmatrix} \tag{60}$$

$$\boldsymbol{C}_c = \begin{pmatrix} 1 & 0 \\ 0 & 1 \end{pmatrix} \tag{61}$$

$$\boldsymbol{D}_c = \begin{pmatrix} 5 & 0 \\ 0 & 2 \end{pmatrix} \tag{62}$$

Note that the disturbances to the oven operation is somehow complicated than usual. The disturbance vector, $\boldsymbol{Z}_c$, is modeled as follows, where the practical intensity of the disturbances is adopted from Lou and Huang [3]:

$$\dot{\boldsymbol{Z}}_c = \boldsymbol{G}_c\boldsymbol{Z}_c + \boldsymbol{H}_c\tilde{\boldsymbol{Z}}_c \tag{63}$$

where

$$\tilde{\boldsymbol{Z}}_c = \begin{pmatrix} \tilde{z}_c^T \\ \tilde{z}_c^P \end{pmatrix} \tag{64}$$

$$\boldsymbol{G}_c = \begin{pmatrix} -0.1 & 0 \\ 0 & -0.1 \end{pmatrix} \tag{65}$$

$$\boldsymbol{H}_c = \begin{pmatrix} 0.1 & 0 \\ 0 & 0.1 \end{pmatrix} \tag{66}$$

4.1.2. Coating quality model

The process output variables (i.e., the panel temperature (or the film temperature), T, and the oven pressure (or the pressure immediately above the coating surface), P) are the product input variables. The product output variables are the crosslinking conversion (x) and the solvent residue in the film (r). Thus, the product model is as follows, where the parameter values in the system matrices are determined by using the data from Lou and Huang [3]:

$$\dot{\boldsymbol{X}}_d = \boldsymbol{A}_d\boldsymbol{X}_d + \boldsymbol{B}_d\boldsymbol{U}_d$$

$$\boldsymbol{Y}_d = \boldsymbol{C}_d\boldsymbol{X}_d + \boldsymbol{D}_d\boldsymbol{Z}_d$$

where

$$\boldsymbol{X}_d = \begin{pmatrix} x \\ r \end{pmatrix} \tag{67}$$

$$\boldsymbol{U}_d = \boldsymbol{Y}_c = \begin{pmatrix} T \\ P \end{pmatrix} \tag{68}$$

$$\boldsymbol{Y}_d = \begin{pmatrix} x \\ r \end{pmatrix} \tag{69}$$

$$\boldsymbol{Z}_d = \begin{pmatrix} z_d^x \\ z_d^r \end{pmatrix} \tag{70}$$

$$\boldsymbol{A}_d = \begin{pmatrix} -0.0042 & 0 \\ 0 & -0.0126 \end{pmatrix} \tag{71}$$

$$\boldsymbol{B}_d = \begin{pmatrix} 8.9632 \times 10^{-5} & 0 \\ -2.3966 \times 10^{-4} & 1.892 \times 10^{-3} \end{pmatrix} \tag{72}$$

$$\boldsymbol{C}_d = \begin{pmatrix} 1 & 0 \\ 0 & 1 \end{pmatrix} \tag{73}$$

$$\boldsymbol{D}_d = \begin{pmatrix} 2 & 0 \\ 0 & 1 \end{pmatrix} \tag{74}$$

According to practical operaiton in the industries, the disturbance vector, $\boldsymbol{Z}_d$, can be modeled as follows:

$$\dot{\boldsymbol{Z}}_d = \boldsymbol{G}_d\boldsymbol{Z}_d + \boldsymbol{H}_d\tilde{\boldsymbol{Z}}_d \tag{75}$$

where

$$\tilde{\boldsymbol{Z}}_d = \begin{pmatrix} \tilde{z}_d^x \\ \tilde{z}_d^r \end{pmatrix} \tag{76}$$

$$\boldsymbol{G}_d = \begin{pmatrix} -0.1 & 0 \\ 0 & -0.01 \end{pmatrix} \tag{77}$$

$$\boldsymbol{H}_d = \begin{pmatrix} 0.05 & 0 \\ 0 & 0.01 \end{pmatrix} \tag{78}$$

4.1.3. Coating quality specification

While there are many coating quality indicators with quality specifications, two of them are selected in this study, i.e., the final crosslinking conversion of at least 90% and the maximum solvent residue of 3% in the coating when a vehicle leaves the curing oven. Note that these coating quality requirements should be guaranteed when the process operation and product manufacturing experience severe disturbances.

4.2. Control system design

The cascade control featured IPPC scheme depicted in Fig. 2 is used to control this integrated oven-baking film-curing system. The IPP controller is designed by following the IPP Controller Gain Matrix Determination (or simply CGMD) procedure that is described in an early section.

4.2.1. Process controller design

The gain matrices, $\boldsymbol{K}_{c_1}$ and $\boldsymbol{K}_{c_2}$, can be determined through implementing the CGMD procedure. They are

$$\boldsymbol{K}_{c_1} = \begin{pmatrix} 43.478 & -1.043 \\ 0 & 0.6 \end{pmatrix} \tag{79}$$

$$\boldsymbol{K}_{c_2} = \begin{pmatrix} 60.770 & -1.458 \\ 0 & 0.838 \end{pmatrix} \tag{80}$$

4.2.2. Product controller design

The product controller should be designed in the same way as that for the process controller design. However, this is computationally more complicated, since the designed closed-loop process control system acts as the "product actuator" of the product system [4]. Therefore, a closed-loop-process-open-loop-product model shown in Eqs. (21) and (22) should be used in the product controller design.

As the first step, the closed-loop-process-open-loop-product model has the following state matrix $\boldsymbol{A}_0$ and the control matrix $\boldsymbol{B}_0$:

$$\boldsymbol{A}_0 = \begin{pmatrix} -0.0023 & 0 & 0.023 & 0.04 & 0 & 0 \\ 0 & -0.0025 & 0 & 1.667 & 0 & 0 \\ -43.339 & 1.040 & -1.398 & -0.0003 & 0 & 0 \\ 0 & -0.60 & 0 & -1.398 & 0 & 0 \\ 0.0001 & 0 & 0 & 0 & -0.0042 & 0 \\ -0.0002 & 0.0019 & 0 & 0 & 0 & -0.0126 \end{pmatrix} \tag{81}$$

$$\boldsymbol{B}_0 = \begin{pmatrix} 0 & 0 \\ 0 & 0 \\ 43.478 & -1.043 \\ 0 & 0.6 \\ 0 & 0 \\ 0 & 0 \end{pmatrix} \tag{82}$$

The preferred state gain matrix, $\boldsymbol{K}_d^p$, is also obtained through executing the preferred state gain matrix design procedure (see, Fig. 4). The resulting product gain matrices are

$$\boldsymbol{K}_{d_1} = \begin{pmatrix} 1.116 \times 10^4 & 0 \\ 1.413 \times 10^3 & 5.285 \times 10^2 \end{pmatrix} \tag{83}$$

$$\boldsymbol{K}_{d_2} = \begin{pmatrix} 2.390 & 0 & 0.016 & 0.028 & 2.996 \times 10^4 & 0 \\ 0.002 & 2.372 & 0 & 1.146 & 3.796 \times 10^3 & 1.405 \times 10^3 \end{pmatrix} \tag{84}$$

4.3. Control performance analysis

The effectiveness of using the IPP controller is demonstrated through comparing the product and process performance with that when only the process controller is used. In the study, various disturbances with different magnitudes and occurrence times are exerted on the process-product system in operation.

4.3.1. System performance under solely process control

Three types of disturbance combinations are considered. They are (a) the process disturbances only, (b) the product disturbances only, and (c) both the process and product disturbances. In each case, a process controller with the control parameters in Eqs. (79) and (80) is used, but the product controller is disconnected (in the open-loop mode). Each case is discussed below.

4.3.1.1. Process disturbances only. There are two types of disturbances: (i) $\tilde{z}_c^T$ that affects the panel temperature (or the film temperature), T, and (ii) $\tilde{z}_c^P$ that affects the oven pressure, P (see Fig. 6(a) and (b)). Fig. 6(c) and (d) show that the oven temperature (T) and the oven pressure (P) are disturbed for a very short period of time after the entering of the disturbances, and then returned to the normal operation quickly. Because of this, the product dynamic performance and thus the final coating quality, in terms of the conversion percentage (x) and the solvent residue (r), are all well acceptable (see Fig. 6(e) and (f)).

4.3.1.2. Product disturbances only. When the disturbances enter the product system which is under open-loop control, the product performance becomes questionable. Fig. 7(a) and (b) plot the disturbances affecting the crosslinking conversion (x) and the solvent residue (r). In this case, the process performance shown in Fig. 7(c) and (d) are perfect. However, the product dynamics given in Fig. 7(e) and (f) are disturbed several times, which makes the final coating quality unacceptable, since the conversion (x) is below the minimum acceptable percentage of 90% and the solvent residue (r) is above the maximum acceptable percentage of 3%. This suggests that the use of the process controller only is insufficient for product quality control.

4.3.1.3. Both process and product disturbances appeared. When both the process and product disturbances enter the entire system (see Fig. 8(a) through (d)), the process dynamics is disturbed but is still well acceptable. As stated before, the process output variables (i.e., the oven temperature (T) and the oven pressure (P)) are the input variables of the product system (i.e., the film temperature (T) and the air pressure just above the film (P)). The fluctuation of the film temperature at the 900th s and that of the pressure at the 600th, 800th, and 1000th s cause the fluctuations of the product controlled variables (i.e., the conversion (x) and the solvent residue (r)) in those time instants. These fluctuations, plus the product disturbances occurred at the 200th s (see Fig. 8(d)) and at the 300th, 500th, and 700th s (see Fig. 8(c)), all influence negatively the product quality

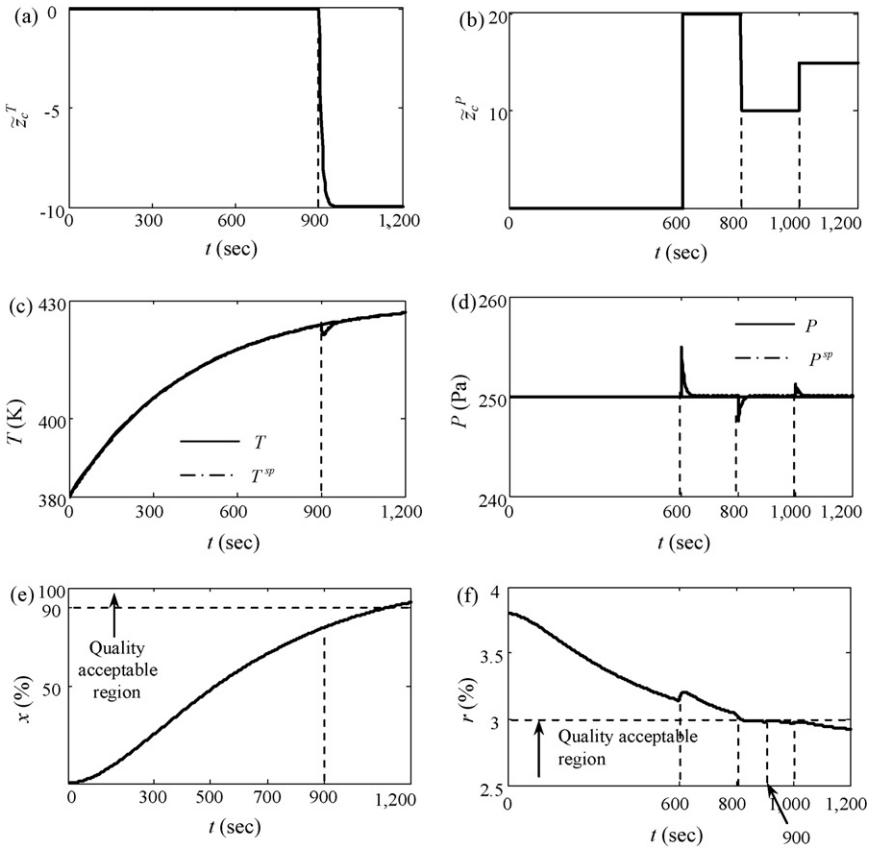

Fig. 6. Process disturbance profiles and system performance when only the process controller is used: (a) the disturbance on the oven temperature, (b) the disturbance on the oven pressure, (c) the oven temperature dynamics, (d) the oven pressure dynamics, (e) the crosslinking conversion dynamics, and (f) the solvent residue dynamics.

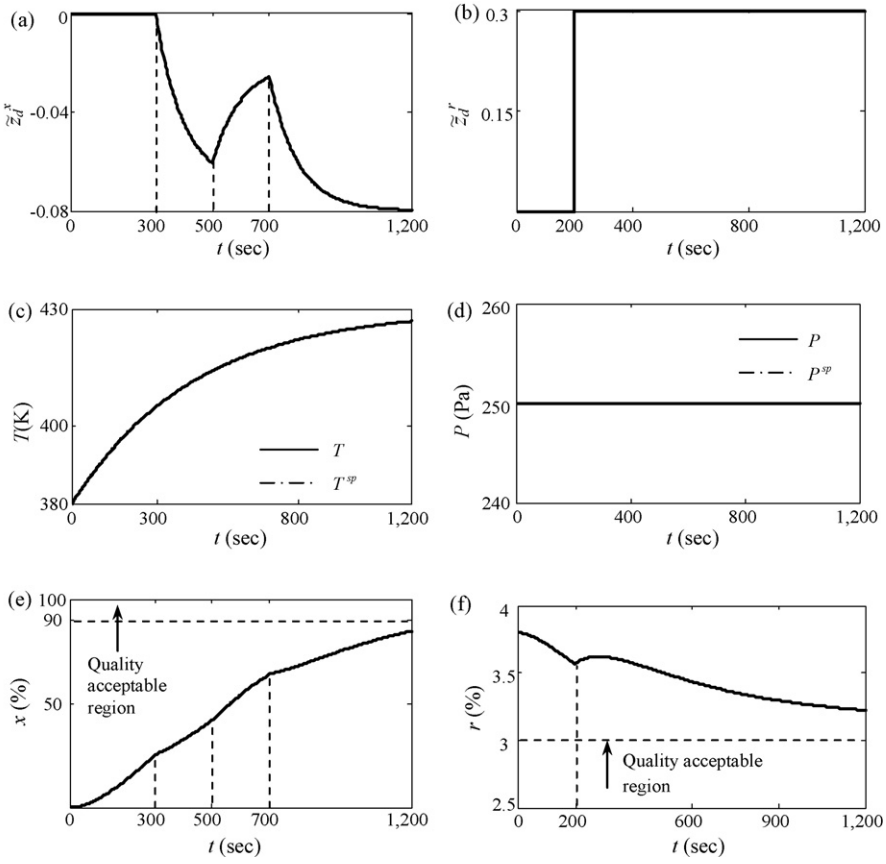

Fig. 7. Product disturbance profiles and system performance when only the process controller is used: (a) the disturbance on the crosslinking conversion, (b) the disturbance on the solvent removal, (c) the oven temperature dynamics, (d) the oven pressure dynamics, (e) the crosslinking conversion dynamics, and (f) the solvent residue dynamics.

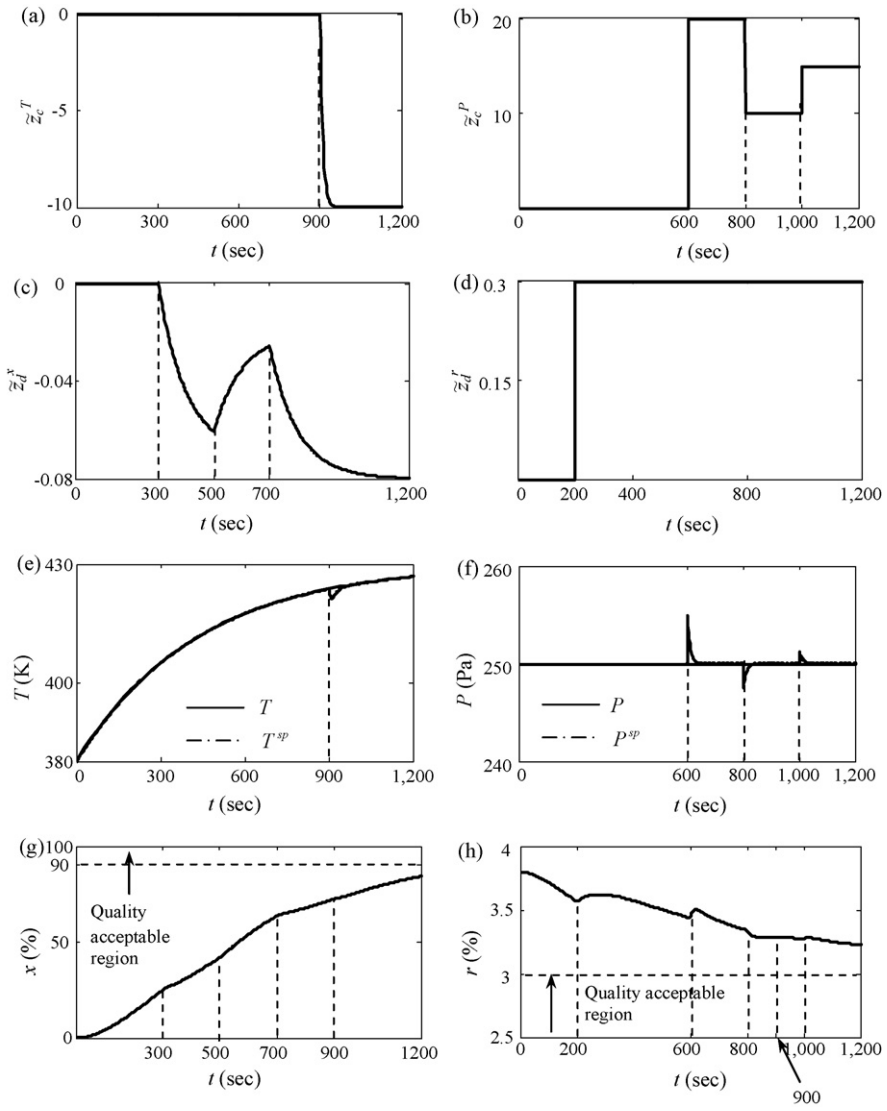

Fig. 8. Process and product disturbance profiles and system performance when only the process controller is used: (a) the disturbance on the oven temperature, (b) the disturbance on the oven pressure, (c) the disturbance on the crosslinking conversion, (d) the disturbance on the solvent removal, (e) the oven temperature dynamics, (f) the oven pressure dynamics, (g) the crosslinking conversion dynamics, and (h) the solvent residue dynamics.

(see the dynamic performance of x and r in Fig. 8(g) and (h)). Finally, the coating quality is unacceptable, as the conversion percentage (x) is only 84.4% and the solvent residue (r) is as high as 3.23%.

4.3.2. System performance under IPP control

The simulation results obtained in the last two cases reveal the followings. (i) The product quality may be affected to some extent when process disturbances enter the process system, even if the process controller acts swiftly and effectively. (ii) When the product disturbances enter the product system, the product quality can be damaged, regardless of how perfect the process control is. (iii) If both the process and product disturbances enter the entire system, product quality can be even worse, no matter how well the process controller can act. The product quality related problems summarized above can be solved by employing the IPP controller. In this study, all the process and product disturbances are considered as the worst case scenario (see, Fig. 9(a)–(d)). As shown in Fig. 9(e) and (f), the set-point of the oven temperature (T^{sp}) and that of the pressure (P^{sp}) of the process can be all dynamically adjusted; note that the dotted curves of T^{sp} and P^{sp} are almost completely overlapped with the solid curves of T and P in the two figures, since the process controller acts nearly perfectly. With the adjusted set-points of T and P, the product controller performs also extremely well, showing a very ideal dynamic behavior of the crosslinking conversion (x) and the solvent residue (r) (see Fig. 9(g) and (h)); these guarantee the achievement of the quality requirement after the curing operation (see x at 92.5% and r at 2.92%).

Another advantage of using the IPP controller is that the product quality can be monitored and controlled throughout the entire manufacturing process. This provides a unique opportunity for process engineers/operators to identify potential quality problems so that quick actions, if necessary, can be taken in the earliest time during operation. Needless to say, such a unique opportunity does not exist for the manufacturing using process control techniques and post-process product quality inspection methods.

Note that the introduced model-based IPPC design approach requires both the process model and the product model highly reliable. In many practical applications, however, the derived process and/product models may show model mismatch in some operational regions. If that is the case, it is suggested to introduce a reference model for the concerned process or product system. It may be also desirable to introduce a system adaptation capacity so that the models used in the IPPC system can be satisfactory. It is worthwhile to note that the well-known internal model control

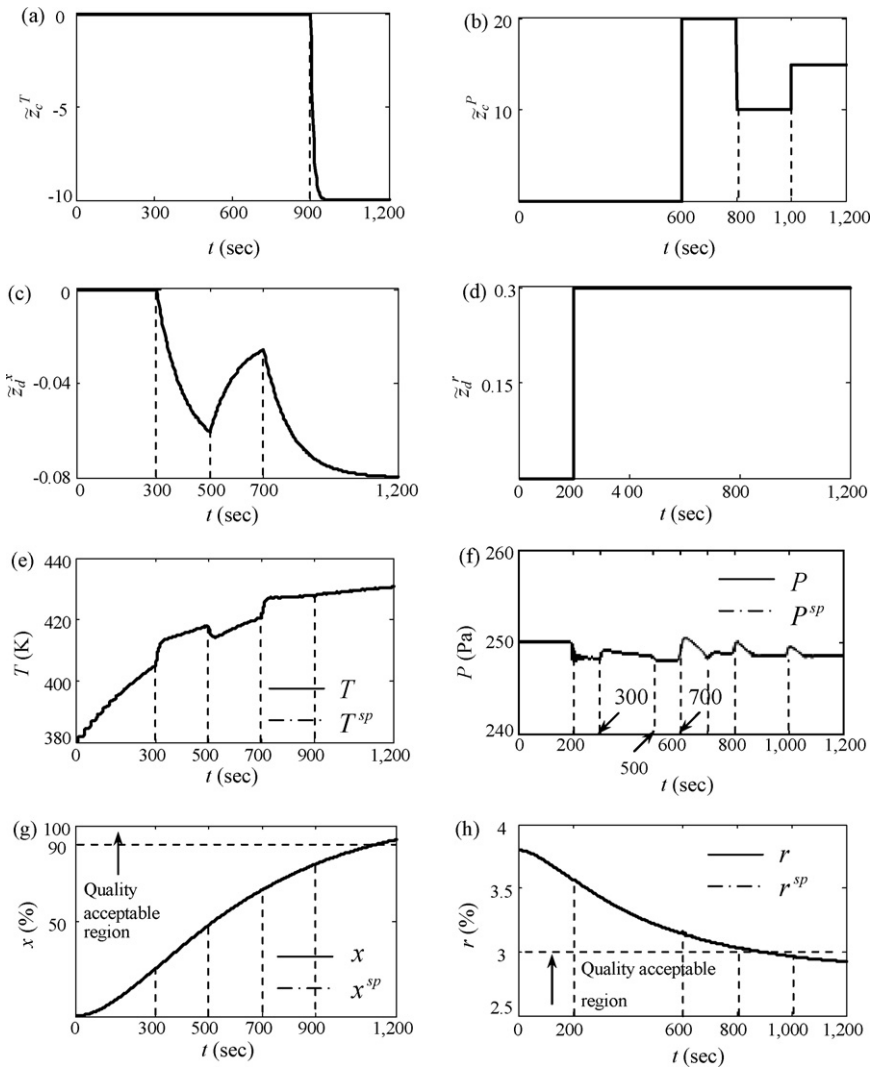

Fig. 9. Process and product disturbance profiles and system performance when the IPP controller is used: (a) the disturbance on the oven temperature, (b) the disturbance on the oven pressure, (c) the disturbance on the crosslinking conversion, (d) the disturbance on the solvent removal, (e) the oven temperature dynamics, (f) the oven pressure dynamics, (g) the crosslinking conversion dynamics, and (h) the solvent residue dynamics.

(IMC) and model predictive control (MPC) design techniques can also be readily integrated in the IPPC system synthesis. This can make the resulting IPPC system more robust in handling model and parametric uncertainties and more predictable in product quality development.

5. Concluding remarks

Traditionally practiced product quality control is solely based on the information obtained from post-production inspection. While always necessary, it is fundamentally reactive as it acts after off-specification and/or defects are identified in the final products. A proactive way of product QC is to identify potential quality problems during product manufacturing and then take immediate action(s) to prevent them from occurrence in the final products. The proactive QC can be most effectively realized through designing an integrated process and product control system.

The IPP control system design methodology introduced in this work is general and simple. It is applicable to any multi-input–multi-output product–process system if it can be characterized by linear models. Note that for a nonlinear system, many techniques are available for linearizing a nonlinear model so that the introduced design methodology can still be satisfactorily used. The case study has demonstrated the efficacy of the design methodology, as it is shown that under the IPP control, the product quality can be effectively controlled when the process system and the product system experience various disturbances of any combinations. A fundamental reason of quality assurance which is also a unique feature of this proactive QC approach is that the set-points of the process control loop are adjusted accordingly based on the product dynamic information obtained during product manufacturing. Therefore, the IPP control is an in-process, “all-time”, “on-aim” proactive QC approach.

It must be pointed out that the use of IPP control is by no means to replace post-process inspection-based QC. Although a large number of quality problems can be effectively prevented during manufacturing when under the IPP control, other quality problems, which are not modeled, could appear in the final products. However, it is evident that IPPC can greatly reduce and simplify the inspection-based QC activities.

Acknowledgments

This work was in part supported by National Science Foundation (CMMI 0700178 and CBET 0730383).

Appendix A. Derivation of the process controller gain matrices

According to Fig. 2, the following relationships hold:

$$\dot{\boldsymbol{e}}_c = \boldsymbol{Y}_c^{sp} - \boldsymbol{Y}_c \tag{A1}$$

$$\boldsymbol{U}_c = \boldsymbol{K}_{c_1}\boldsymbol{e}_c - \boldsymbol{K}_{c_2}\boldsymbol{X}_c \tag{A2}$$

Taking derivative of Eq. (A2) and then substituting Eqs. (7) and (A1) into it yield,

$$\dot{\boldsymbol{U}}_c = -(\boldsymbol{K}_{c_1}\boldsymbol{C}_c + \boldsymbol{K}_{c_2}\boldsymbol{A}_c)\boldsymbol{X}_c - \boldsymbol{K}_{c_2}\boldsymbol{B}_c\boldsymbol{U}_c + \boldsymbol{K}_{c_1}\boldsymbol{Y}_c^{sp} - \boldsymbol{K}_{c_1}\boldsymbol{D}_c\boldsymbol{Z}_c \tag{A3}$$

where $\boldsymbol{K}_{c_1}$ $(m\times m)$ and $\boldsymbol{K}_{c_2}$ $(m\times n)$ are the controller gain matrices to be determined.

By grouping Eqs. (7) and (A3), an augmented system model can be obtained, i.e.,

$$\begin{pmatrix}\dot{\boldsymbol{X}}_c\\ \dot{\boldsymbol{U}}_c\end{pmatrix} = \begin{pmatrix}\boldsymbol{A}_c & \boldsymbol{B}_c\\ -(\boldsymbol{K}_{c_1}\boldsymbol{C}_c + \boldsymbol{K}_{c_2}\boldsymbol{A}_c) & -\boldsymbol{K}_{c_2}\boldsymbol{B}_c\end{pmatrix}\begin{pmatrix}\boldsymbol{X}_c\\ \boldsymbol{U}_c\end{pmatrix} + \begin{pmatrix}\boldsymbol{0}\\ \boldsymbol{K}_{c_1}\end{pmatrix}\begin{pmatrix}\boldsymbol{Y}_c^{sp} & -\boldsymbol{D}_c\boldsymbol{Z}_c\end{pmatrix} \tag{A4}$$

In the above model, the closed-loop stability and transient response performance are governed by the $n+m$ eigenvalues of the closed-loop system matrix $((n+m)\times(n+m))$, which can be decomposed as

$$\begin{pmatrix}\boldsymbol{A}_c & \boldsymbol{B}_c\\ -(\boldsymbol{K}_{c_1}\boldsymbol{C}_c + \boldsymbol{K}_{c_2}\boldsymbol{A}_c) & -\boldsymbol{K}_{c_2}\boldsymbol{B}_c\end{pmatrix} = \begin{pmatrix}\boldsymbol{A}_c & \boldsymbol{B}_c\\ 0 & 0\end{pmatrix} - \begin{pmatrix}0\\ \boldsymbol{I}_m\end{pmatrix}\begin{pmatrix}\boldsymbol{K}_{c_1}\boldsymbol{C}_c + \boldsymbol{K}_{c_2}\boldsymbol{A}_c & \boldsymbol{K}_{c_2}\boldsymbol{B}_c\end{pmatrix} \tag{A5}$$

With Eq. (A5), Eq. (A4) can be rewritten as

$$\dot{\boldsymbol{\Psi}}_c = (\boldsymbol{\Lambda}_c - \boldsymbol{\Gamma}_c\boldsymbol{K}_c^p)\boldsymbol{\Psi}_c + \boldsymbol{\Gamma}_c\boldsymbol{\Phi}_c^{sp} \tag{A6}$$

Note that variables and parametric matrices in the above equation are defined in Eqs. (13) through (17). Also note that the system output model has shown in Eqs. (18) and (19). According to Eq. (17), the controller gain matrices can be evaluated by

$$\begin{pmatrix}\boldsymbol{K}_{c_1} & \boldsymbol{K}_{c_2}\end{pmatrix} = \boldsymbol{K}_c^p\begin{pmatrix}\boldsymbol{C}_c & 0\\ \boldsymbol{A}_c & \boldsymbol{B}_c\end{pmatrix}^{-1}$$

Appendix B. Derivation of the product controller gain matrices

Let the overall system in Fig. 2 be controllable. Then the following relationships hold:

$$\dot{\boldsymbol{e}}_o = \boldsymbol{Y}_o^{sp} - \boldsymbol{Y}_o \tag{B1}$$

$$\boldsymbol{U}_o = \boldsymbol{K}_{d_1}\boldsymbol{e}_o - \boldsymbol{K}_{d_2}\boldsymbol{X}_o \tag{B2}$$

Taking derivative of Eq. (B2) and utilizing Eqs. (21) and (B1) gives,

$$\dot{\boldsymbol{U}}_o = -(\boldsymbol{K}_{d_1}\boldsymbol{C}_o + \boldsymbol{K}_{d_2}\boldsymbol{A}_o)\boldsymbol{X}_o - \boldsymbol{K}_{d_2}\boldsymbol{B}_o\boldsymbol{U}_o + \boldsymbol{K}_{d_1}\boldsymbol{Y}_o^{sp} - \boldsymbol{K}_{d_1}\boldsymbol{D}_o\boldsymbol{Z}_o - \boldsymbol{K}_{d_2}\boldsymbol{E}_o\boldsymbol{Z}_c \tag{B3}$$

where $\boldsymbol{K}_{d_1}$ $(m\times m)$ and $\boldsymbol{K}_{d_2}$ $(m\times(n+m+l))$ are the product controller gain matrices.

By combining Eqs. (21) and (B3), the augmented product–process model is obtained below:

$$\begin{pmatrix}\dot{\boldsymbol{X}}_o\\ \dot{\boldsymbol{U}}_o\end{pmatrix} = \begin{pmatrix}\boldsymbol{A}_o & \boldsymbol{B}_o\\ -(\boldsymbol{K}_{d_1}\boldsymbol{C}_o + \boldsymbol{K}_{d_2}\boldsymbol{A}_o) & -\boldsymbol{K}_{d_2}\boldsymbol{B}_o\end{pmatrix}\begin{pmatrix}\boldsymbol{X}_o\\ \boldsymbol{U}_o\end{pmatrix} + \begin{pmatrix}\boldsymbol{0}\\ \boldsymbol{K}_{d_1}\end{pmatrix}(\boldsymbol{Y}_o^{sp} - \boldsymbol{D}_o\boldsymbol{Z}_o) + \begin{pmatrix}\boldsymbol{E}_o\\ -\boldsymbol{K}_{d_2}\boldsymbol{E}_o\end{pmatrix}\boldsymbol{Z}_c \tag{B4}$$

The closed-loop system model (i.e., Eqs. (B4) and (22)) can be rewritten as

$$\dot{\boldsymbol{\Psi}}_d = (\boldsymbol{\Lambda}_d - \boldsymbol{\Gamma}_d\boldsymbol{K}_d^{\boldsymbol{p}})\boldsymbol{\Psi}_d + \boldsymbol{\Gamma}_d\boldsymbol{\Phi}_d^{sp} + \boldsymbol{E}_d\boldsymbol{Z}_c \tag{B5}$$

$$\boldsymbol{Y}_d = \boldsymbol{\Omega}_d\boldsymbol{\Psi}_d + \boldsymbol{D}_d\boldsymbol{Z}_d \tag{B6}$$

where

$$\boldsymbol{\Psi}_d = \begin{pmatrix}\boldsymbol{X}_o\\ \boldsymbol{U}_o\end{pmatrix} \tag{B7}$$

$$\boldsymbol{\Phi}_d^{sp} = \boldsymbol{K}_{d_1}\begin{pmatrix}\boldsymbol{I}_m & -\boldsymbol{D}_o\end{pmatrix}\begin{pmatrix}\boldsymbol{Y}_o^{sp}\\ \boldsymbol{Z}_o\end{pmatrix} \tag{B8}$$

$$\boldsymbol{\Lambda}_d = \begin{pmatrix}\boldsymbol{A}_o & \boldsymbol{B}_o\\ 0 & 0\end{pmatrix} \tag{B9}$$

$$\boldsymbol{\Gamma}_d = \begin{pmatrix}0\\ \boldsymbol{I}_m\end{pmatrix} \tag{B10}$$

$$\boldsymbol{K}_d^p = \begin{pmatrix}\boldsymbol{K}_{d_1}\boldsymbol{C}_o + \boldsymbol{K}_{d_2}\boldsymbol{A}_o & \boldsymbol{K}_{d_2}\boldsymbol{B}_o\end{pmatrix} \tag{B11}$$

$$\boldsymbol{E}_d = \begin{pmatrix}\boldsymbol{E}_o\\ -\boldsymbol{K}_{d_2}\boldsymbol{E}_o\end{pmatrix} \tag{B12}$$

$$\boldsymbol{\Omega}_d = \begin{pmatrix}\boldsymbol{C}_o & 0\end{pmatrix} \tag{B13}$$

According to Eq. (B11), the controller gain matrices can be evaluated by:

$$\begin{pmatrix}\boldsymbol{K}_{d_1} & \boldsymbol{K}_{d_2}\end{pmatrix} = \boldsymbol{K}_d^p\begin{pmatrix}\boldsymbol{C}_o & \boldsymbol{0}\\ \boldsymbol{A}_o & \boldsymbol{B}_o\end{pmatrix}^{-1}$$

References

[1] S.M. Wu, J. Ni, S. Hu, Next generation quality control in manufacturing real time defect prevention, in: Proceedings of the ASME Winter Annual Meeting, San Francisco, CA, 1989.
[2] Y. Yabuki, J.F. MacGregor, Product quality control in semibatch reactors using midcourse correction policies, Ind. Eng. Chem. Res. 36 (1997) 1268–1275.
[3] H.H. Lou, Y.L. Huang, Integrated modeling and simulation for improved reactive drying of clearcoat, Ind. Eng. Chem. Res. 38 (2000) 500–507.
[4] J. Xiao, Y. Qian, H.H. Lou, Y.L. Huang, Integrated product and process control of single-input–single-output systems, AIChE J. 53 (2007) 891–901.
[5] W.L. Brogan, Modern Control Theory, Prentice-Hall, New Jersey, 1991.
[6] B.W. Bequette, Process Control, Prentice-Hall, New Jersey, 2003.
[7] D.B. Miron, Design of Feedback Control Systems, Harcourt Vrace Jovanovich, New York, 1989.
[8] C.D. Richard, H.B. Robert, Modern Control Systems, Prentice-Hall, New Jersey, 2001.
[9] R.A. Dickie, D.R. Bauer, S.M. Ward, D.A. Wagner, Modeling paint and adhesive cure in automotive applications, Prog. Org. Coat. 31 (1997) 209–216.
[10] S.S. Peng, Optimizing airflow reversals for kiln drying of softwood timber by applying mathematical models, Maderas, Cienc. Technol. 6 (2004) 95–108.